

## Effect of Subpin Feedback in coupled MCNP6/CTF

Alexander Bennett, Maria Avramova, Kostadin Ivanov

Department of Nuclear Engineering, North Carolina State University, 2500 Stinson Drive, 3140 Burlington Engineering Labs, Raleigh, NC 27695

asbenne3@ncsu.edu, mnavramo@ncsu.edu, knivanov@ncsu.edu

**Abstract** - There has been a trend towards coupled Monte Carlo (MC) neutronic and Thermal Hydraulic (TH) subchannel codes to be used to create reference solutions. Typically the pin average feedback assumption is used to decrease the computational requirements. The pin average feedback assumption is where the fuel region in the neutronics code is modeled as a single region. In this paper the number of subpin fuel regions are varied in a coupled MC neutronics and TH subchannel code to get a measure of their effect on a coupled solution as well as to verify the pin average feedback assumption. The pin average feedback assumption was found to give errors of over 100 pcm and over 15% in the fuel centerline temperature. For most of the cases, decreasing the number of subpin regions in MCNP6 gave conservative results, while decreasing the number of subpin regions in CTF gave non conservative results, with an exception of the eigenvalue. The effect on the eigenvalue was reversed.

## I INTRODUCTION

There has been a recent trend towards high fidelity multiphysics codes to get accurate reactor core solutions. This trend has been driven by the need for more reference solutions for reactors. For each new reactor design, the computational tools used for core design need to be validated with reference solutions at different conditions. Traditionally the reference solutions have come from experiments. Performing experiments to get detailed information during reactor operation is very difficult and costly. With the increase of computational power, high fidelity multiphysics codes are starting to be seen as an alternative solution to get reference solutions. To be able to produce reference solutions, these high fidelity multiphysics codes must be able to produce accurate results with minimal assumptions.

One type of high fidelity multiphysics code is a coupled MC Neutronics and TH subchannel code. The advantage of using a MC Neutronics code is exact geometry modeling and the use of continuous energy cross sections. Coupling the MC Neutronics code with a TH subchannel code allows for accurate modeling of the feedback effects. One of the disadvantages of this type of coupled code is the large amount of computational time. A common assumption that is used to decrease the computational time is to model the fuel in the MC Neutronics code as a single region in the radial direction ([1, 2, 3]). The pin average feedback assumption removes the temperature and power gradient radially in the fuel during the Neutronics calculations. This will then affect the fuel centerline temperature, self shielding, shape of gadolinium burnout, etc. This assumption could effect the accuracy of the coupled code.

The purpose of this paper is to evaluate the effect that subpin feedback has on the results, which will give some insight into the effect of the pin average feedback assumption. The effect of subpin feedback is studied using a coupled MCNP6/CTF code, where MCNP6 is a MC Neutronics code and CTF is a TH subchannel code. In this study the number of subpin fuel regions are varied in both codes.

The computer codes used in the coupled MCNP6/CTF code are described in Section II and the coupling scheme is described in Section III. The geometry that this study is performed on is described in Section IV. The results of this study are given in Section V.

## II COMPUTER CODES

The coupled code used in this study includes the MC Neutronics code MCNP6 and the TH subchannel code CTF. Additionally the codes FIT\_OTF and MAKXSF are used in the cross section generation which are included with MCNP6.

### 1 MCNP6

The MC Neutronics code MCNP6 [4] stands for Monte Carlo N-Particle. MCNP6 is a three-dimensional (3D) general purpose MC transport code that solves the integral transport equation. Some of the advantages of MCNP6 is that it has exact geometry modeling, uses continuous energy cross sections, incorporates features supporting TH feedback, includes options for burnup/depletion calculations, and can be run in parallel with OpenMP and/or MPI. Within the coupled code, MCNP6 is used to calculate the power distribution and the eigenvalue. The power distribution can be calculated with either cell tallies or mesh tallies. In the coupling scheme, which is described in Section III, requires that cell tallies are used to calculate the power distribution. The cell tallies are track length estimators and are calculated as:

$$\phi = \frac{1}{v \cdot W} \sum_{i \in \text{particles}} w_i \cdot d_i \quad (1)$$

where  $V$  is the cell volume,  $W$  is the total source weight,  $w_i$  is the weight of particle  $i$ , and  $d_i$  is the distance traveled by particle  $i$ .

### A FIT\_OTF

The FIT\_OTF[5] code is used to create On-The-Fly cross sections in MCNP6. The FIT\_OTF code functionalizes the

cross section in energy and temperature. The functionalization is done by creating up to a 17 term expansion of the cross section in temperature. These cross sections can be used over the temperature range from 250K to 3200K. The On-The-Fly cross sections have a fractional tolerance of 0.1% [5] to the actual cross section but add around 10% to 15% [5] additional computational time. The main advantage of using these cross sections is that only one cross section file is needed for each isotope rather than creating a new cross section file at each temperature of interest and for each isotope.

### B MAKXSF

The double differential scattering cross sections or the thermal scattering cross sections are not created by the FIT\_OTF code. Instead, the thermal scattering cross sections are created using the MAKXSF [6] code. The program manipulates cross section libraries for MCNP. Some of the capabilities of MAKXSF include: doppler broadening of resolved cross section data, interpolating thermal scattering kernels and interpolating unresolved resonance cross section data between two temperatures. For the coupled code, MAKXSF is used to create new thermal scattering libraries at various temperatures.

### 2 CTF

CTF [7] is the improved RDFMG (Reactor Dynamics and Fuel Modeling Group, NCSU) version of COBRA-TF. COBRA-TF stands for Coolant Boiling in Rod Arrays-Two Fluid. CTF is a 3D TH simulation code that is designed for LWR vessel and core analysis. CTF uses a two-fluid, three-field modeling approach and solves the mass, momentum, and conservation equations. An advantage of CTF is that it is a two fluid code, it can model both Pressure Water Reactor (PWR) and Boiling Water Reactor (BWR) conditions. Additional modeling advantages include a three-field representation of vapor, continuous liquid, and liquid droplets, as well as the ability to fully model the 3D heat conduction, and the dynamic gap conduction. Recent improvements within CASL have included development of models, enhancing computational efficiency, extensive verification, validation, and uncertainty quantification as well as improving software quality and documentation of CTF. In the radial plane, CTF can model the subchannels using either subchannel centered subchannel or a rod centered subchannel.

### III COUPLING SCHEME

The multiphysics code that is used for this study is the coupled MCNP6/CTF code. Some of the previous work done on this code includes code to code comparisons, assembly level test problems, and an acceleration technique. This information can be found in [8]. A description of the coupled code is also given here. The geometry mapping is described in 1, the temperature dependence on the cross sections is handled as described in 2, the calculation process is described in 3, and the coupling method is described in 4.

### 1 Geometry Mapping

It is important to have the feedback parameters accurately mapped between the two codes. In this coupled code, this is achieved by having MCNP6 model the exact same geometry that CTF uses. This simplifies the geometry mapping process and removes the possibility of adding an additional error from converting from one mesh grid to another. There is one portion of the mesh that MCNP6 does not model with the exact same geometry as CTF and that is the subpin mesh. The coupling is set up so that MCNP6's subpin mesh is uniform in the radial direction. The subpin mesh in CTF is also uniform in the radial direction but the outer most fuel region is half of the radial width than the other fuel regions. The coupling is set up to allow a different number of subpin regions to be specified in each code which requires a mesh conversion between one grid to another whether or not the same type of mesh is used.

To convert from one subpin mesh to another an area averaging technique is used and can be calculated as:

$$Q_{n,r} = \frac{1}{A_{n,r}} \sum_{i \in r} A_{o,i} Q_{o,r} \quad (2)$$

where:

- $Q$  is the quantity of interest (power or temperature)
- $A$  is the area of a subpin region
- $n$  is the new mesh that is being converted to
- $o$  is the original mesh that is being converted from
- $r$  is the radial position in the new mesh
- $i$  is the radial position in the original mesh

This technique is used to keep consistency with how the pin average feedback is already calculated in CTF and to not make any assumption about the shape function.

The rest geometry mapping is carried out is through additional options on the cells cards as well as a numbering scheme for the tally cards in the MCNP input file. The advantage of this type of geometry mapping is that the generality of MCNP is kept and nothing is assumed about the geometry. The disadvantage of this type of geometry mapping is that the MCNP input file becomes very lengthy.

### 2 Temperature Dependence

To accurately account for the temperature dependence within MCNP6, both the single differential and double differential cross section have to be broadened to the correct temperatures. The single differential cross sections are handled by FIT\_OTF. The cross sections created by FIT\_OTF using up to a 17 term expansion, with an energy grid of 50K and a temperature grid of 10K, can have a fraction tolerance of 0.1% [5] to the actual cross sections. For this study, the energy grid was refined to 10K, the temperature grid was refined to 2K, and the functional expansion was allowed to go up to 17 terms. At the time the coupling was created, the double

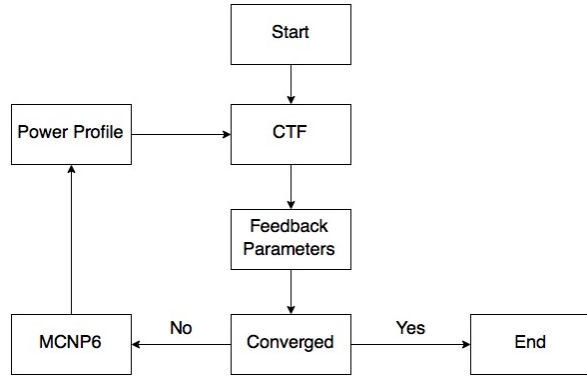


Fig. 1: Flow Chart of the Coupled MCNP6/CTF Code

differential cross sections could not be represented as a functional expansion in MCNP6. Instead, the double differential cross sections are handled by MAKXSF. The MAKXSF code is used to create the thermal scattering cross sections every 1K over the temperature range of the moderator. This does not add a large amount of cross section files since the temperature range of the moderator is only about 10K to 30K for Light Water Reactors (LWR).

### 3 Coupled Calculation

The flow chart of the coupled calculation is shown in Fig. 1. The calculation is started with CTF. The user specifies an initial power distribution. It is important to specify the initial power distribution as close as possible to the final power distribution as it will decrease the computational time needed. If this is not the first iteration, the power distribution is obtained from the previous MCNP6 calculation. After the CTF calculation has been performed, the TH feedback parameters are obtained. The TH feedback parameters include the temperature of the fuel, cladding, and moderator, as well as the density of the moderator. The coupled code then checks the convergence as:

$$\epsilon \leq \max_{i,j} \left| \frac{T_{i,j}^{current} - T_{i,j}^{previous}}{T_{i,j}^{previous}} \right| \quad (3)$$

where  $\epsilon$  is the specified convergence criteria,  $T_{i,j}$  is the temperature in Kelvin for rod/subchannel  $i$  and axial node  $j$ . If this equation is true for all rods and subchannels at each axial level than convergence has been met and the calculation is over. If this equation is false, then MCNP6 is run with the new feedback parameters. MCNP6 calculates a new power distribution which is then passed to CTF to start a new coupled iteration.

### 4 Coupling Method

The coupled MCNP6/CTF code is coupled internally with the CTF source added as folder in the MCNP6 source. For this coupling, code modification had to be made to both codes and an interface layer was created. In MCNP6, a coupling interface had to be created which could update the temperatures and densities of the cell cards and retrieve the power

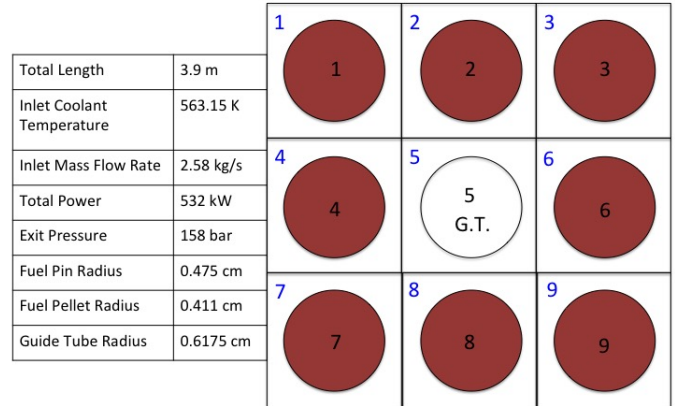


Fig. 2: PWR Mini Assembly

distribution. The interface also contained subroutines that could reset and start a new MCNP6 calculation for each new iteration. In CTF, a coupling interface was already set up but it did not include functions for the subpin distribution. The coupling interface was updated with functions that could retrieve the subpin temperature distribution and could update the subpin power distribution. The interface layer was created to be able to interact with the coupling interfaces of both codes and iterate between them until the convergence criterion is met. The interface layer was also created with additional subroutines to create simplified output files.

## IV GEOMETRY

The geometry that is used in this study is a 3X3 PWR mini assembly. The specifications of this mini assembly are given in Fig. 2. A simple geometry was chosen to allow for lower errors on the tally results. This geometry is based on the benchmark problem in [9], but the number of axial regions is refined from 10 regions to 30 regions. The number of radial regions is varied in both MCNP6 and CTF for the study. The MCNP6 geometry with 1 radial fuel region is shown in Fig. 3, and with 10 radial fuel regions in Fig. 4.

## V RESULTS

In this study, the number of subpin regions are varied in both MCNP6 and CTF. The different radial geometry variations are shown in Table I. Varying the number of subpin regions in MCNP6 gives an insight into the pin average feedback assumption as well as the effect of increasing the number of feedback regions in MCNP6. The pin average feedback assumption corresponds to 1 subpin region in MCNP6. Varying the number of subpin regions in CTF gives an insight into the effect that the number of subpin regions in CTF has on the coupled solution.

The convergence criterion for the coupled code for all of the cases is set to 0.06. To converge the Shannon entropy (source distribution), 200 inactive cycles are run for all of the test cases. To be able to have a good comparison of the

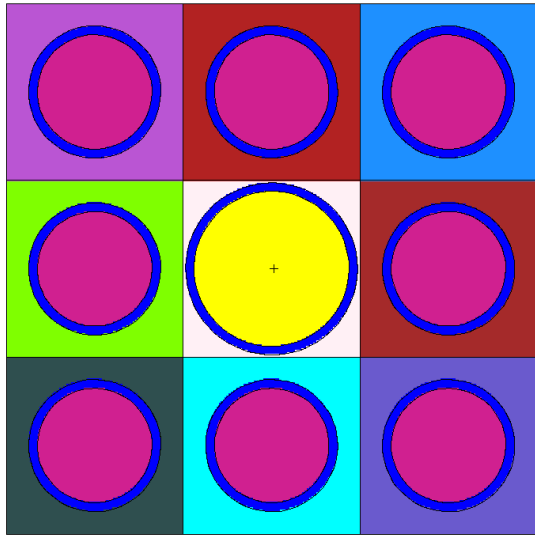


Fig. 3: MCNP Geometry with 1 Radial Fuel Region

| MCNP6 Regions | CTF Regions |
|---------------|-------------|
| 1             | 10          |
| 3             | 10          |
| 5             | 10          |
| 7             | 10          |
| 9             | 10          |
| 10            | 3           |
| 10            | 5           |
| 10            | 7           |
| 10            | 9           |
| 10            | 10          |

TABLE I: Radial Geometry Variations

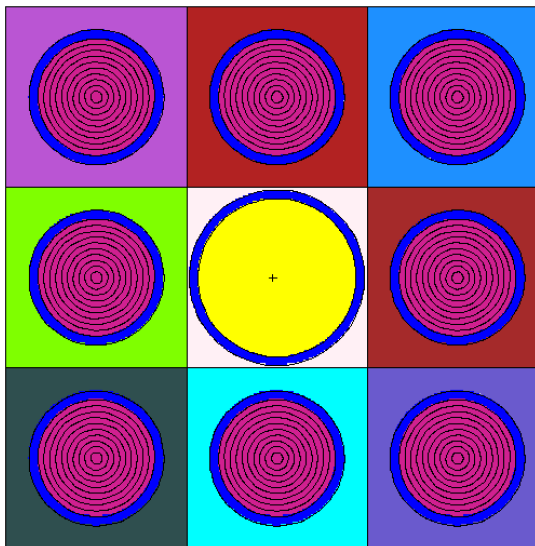


Fig. 4: MCNP Geometry with 10 Radial Fuel Region

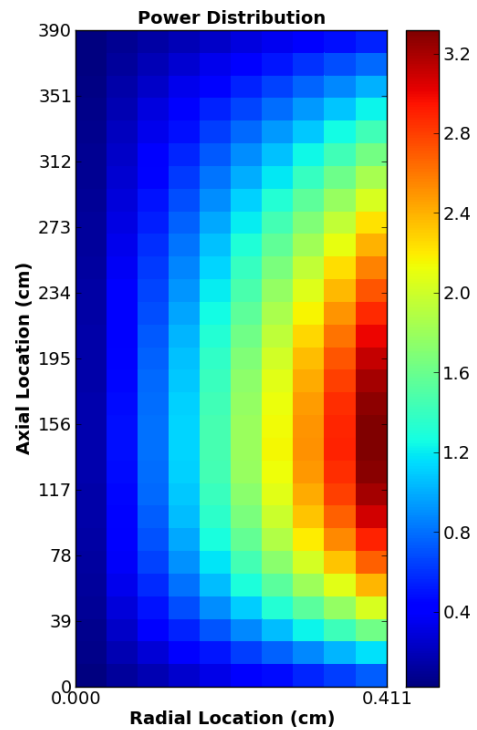


Fig. 5: Power Distribution for Pin 1

computational time across all of the test cases, each MCNP6 calculation is run until the maximum error over all tallies is equal to 0.03. Each cycle in MCNP6 is run with 200,000 particles. For the computational time comparison, all of the cases are run on 8 cores (3.6 GHz).

The reference calculation for all of these cases is the most refined mesh which corresponds to 10 subpin regions in both MCNP6 and CTF. For the reference calculation, the plot of the power distribution for Pin 1 (top left pin) is shown in Fig. 5. The highest power is in the middle of the pin axially and at the outer edge of the pin. This distribution is expected since this is where most of the fissions occur. The plot of the temperature distribution for Pin 1 shown in Fig. 6. The highest temperature is in the middle of the pin axially and radially. All of the following comparisons are made as a percent difference to this case.

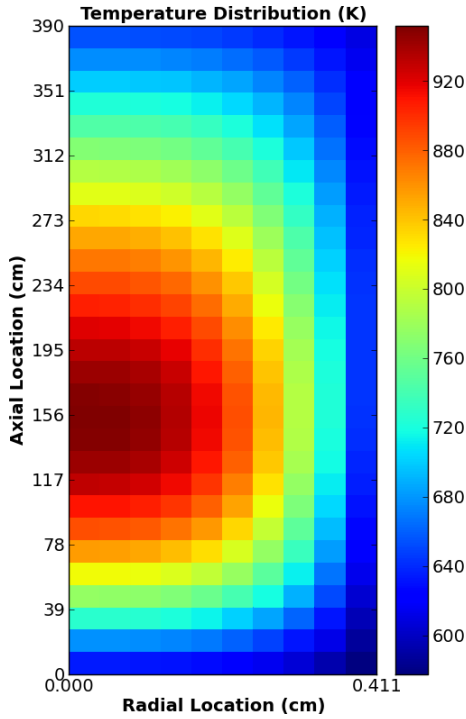


Fig. 6: Temperature Distribution for Pin 1

The maximum difference in the average power distribution is shown in Fig. 7. The term average power corresponds to the average power in the radial different for each pin and axial layer. CTF underestimates the average power distribution for just a few subpin regions while MCNP6 overestimates it. The maximum difference in the average fuel temperature distribution is shown in Fig. 8. Similar to the differences for the average power, CTF underestimates the average fuel temperature while MCNP6 overestimates the average fuel temperature distribution. The maximum difference in the fuel centerline temperature is shown in Fig. 9. Once again, CTF underestimates the results and MCNP6 underestimates the results. The difference in the eigenvalue is shown in Fig. 10. Opposite from the other results, CTF overestimates the eigenvalue and MCNP6 underestimates the eigenvalue. The opposite results for the fuel temperature is expected due to the doppler effect.

From these results, it can be observed that using a single subpin region in MCNP6 or 3 subpin regions in CTF gives large differences. For most of the cases, except for the eigenvalue, decreasing the number of subpin regions in MCNP6 gives conservative results while decrease the number of subpin regions in CTF gives non conservative results. Another interesting result for most of the cases, is that decreasing the number of regions in MCNP6 and CTF had opposite effects on the results. This could lead to a cancellation of some of the errors.

Transitioning to a finer mesh normally gives more accurate results, but also normally requires higher computational requirements. The time (real time) per coupled iteration is shown in Fig. 11. Changing the number of regions in CTF does not have much of an effect on the computational time.

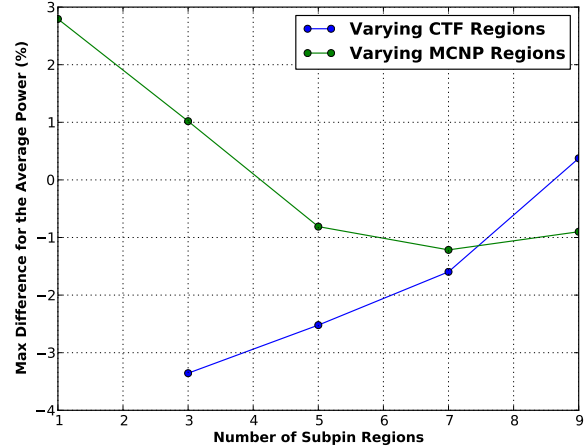


Fig. 7: Max Difference for the Average Power Distribution

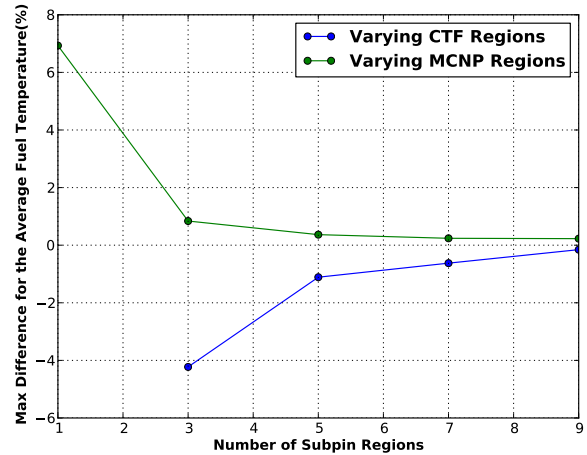


Fig. 8: Max Difference for the Average Fuel Temperature Distribution

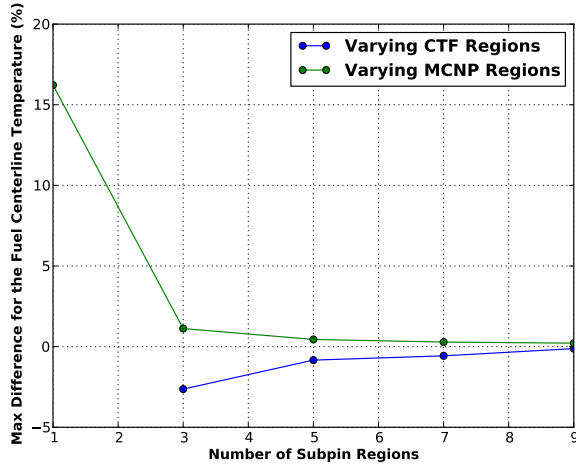


Fig. 9: Max Difference for the Fuel Centerline Temperature Power

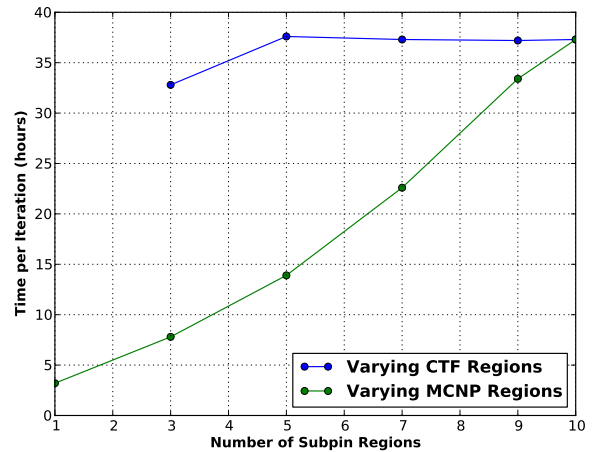


Fig. 11: Time (real time) per Coupled Iteration

This is expected since most of the computational time goes to MCNP6. Increasing the number of regions in MCNP6 increased the computational time almost linearly. For this simple geometry, the time for the most refined cases were over a week. Additional computational information about these cases is given in Table II.

## VI CONCLUSION

In this paper the number of subpin regions modeled in a coupled MC neutronics and TH subchannel code are varied. When the neutronics code was modeled with a single subpin region, which corresponds to the pin average feedback assumption, differences of over 100 pcm and over 15% in the fuel centerline temperature were found. Modeling the TH code with only three subpin regions led to differences over 80 pcm. For most of the cases, decreasing the number of subpin regions in MCNP6 gave conservative results, while decrease the number of subpin regions in CTF gave non conservative results, except for the eigenvalue. For the eigenvalue, decreasing the number of subpin regions in CTF gave conservative results, while decreasing the number of subpin regions in MCNP6 gave non conservative results. Also for most of the results, decreasing the number of subpin regions in MCNP6 and CTF gave opposite effects on the results. Increasing the number of subpin regions in CTF had very little effect on the computational time while increasing the number of subpin regions in MCNP6 gave almost a linear increase with the computational time.

## REFERENCES

1. F. ESPEL, *High Accuracy Modeling for Advanced Nuclear Reactor Core Designs using Monte Carlo based Coupled Calculations*, Ph.D. thesis, The Pennsylvania State University (August 2010).
2. A. IVANOV, *High Fidelity Monte Carlo Based Reactor Physics Calculations*, Ph.D. thesis, Karlsruhe Institute of Technology (2015).
3. W. BERNNAT, N. GUILLIARD, and J. LAPINS, "Monte

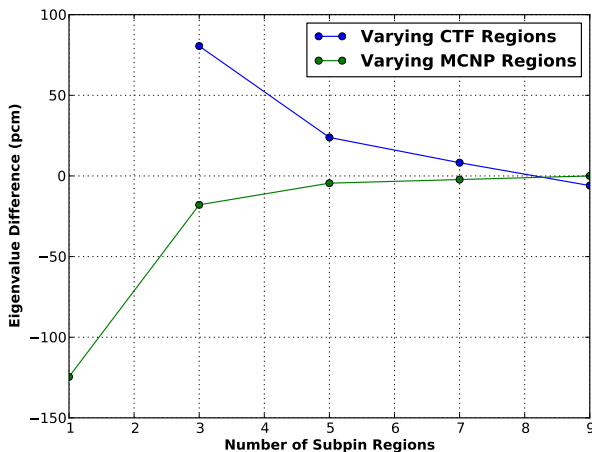


Fig. 10: Eigenvalue Difference

| Regions |     | Total Particles | Total Time (hours) | Time/Iteration (hours) | Iterations |
|---------|-----|-----------------|--------------------|------------------------|------------|
| MCNP6   | CTF |                 |                    |                        |            |
| 1       | 10  | 800             | 15.9               | 3.2                    | 5          |
| 3       | 10  | 1500            | 31.0               | 7.8                    | 4          |
| 5       | 10  | 2200            | 55.6               | 13.9                   | 4          |
| 7       | 10  | 3000            | 113.1              | 22.6                   | 5          |
| 9       | 10  | 3700            | 100.2              | 33.4                   | 3          |
| 10      | 3   | 4000            | 131.0              | 32.8                   | 4          |
| 10      | 5   | 4000            | 150.2              | 37.6                   | 4          |
| 10      | 7   | 4000            | 186.7              | 37.3                   | 5          |
| 10      | 9   | 4000            | 185.9              | 37.2                   | 5          |
| 10      | 10  | 4000            | 149.3              | 37.3                   | 4          |

TABLE II: Computational Information

Carlo Full Core Neutronics Analysis with Detailed Consideration of Thermal-Hydraulic Parameters,” *Joint Int. Conf. on Mathematics and Computational Methods* (2015).

4. J. T. GOORLEY ET AL., “Initial MCNP6 Release Overview,” Tech. Rep. la-ur-13-22934, Los Alamos National Labs (2013).
5. W. R. MARTIN, S. WILDERMAN, F. B. BROWN, and G. YESILYURT, “Implementation of On-The-Fly Doppler Broadening in MCNP,” Tech. Rep. la-ur-13-20662, Los Alamos National Labs (2013).
6. F. B. BROWN, “The makxs code with Doppler Broadening,” Tech. Rep. la-ur-06-7002, Los Alamos National Labs (2006).
7. R. K. SALKO and M. N. AVRAMOVA, *CTF Theory Manual*, RDFMG, NCSU (2016).
8. A. BENNETT, M. AVRAMOVA, and K. IVANOV, “Coupled MCNP6/CTF code: Development, testing, and application,” *Annals of Nuclear Energy*, **96** (2016).
9. A. IVANOV, V. SANCHEZ, R. STIEGLITZ, and K. IVANOV, “High fidelity simulation of conventional and innovative LWR with the coupled Monte-Carlo thermal-hydraulic system MCNP-SUBCHANFLOW,” *Nuclear Engineering and Design*, **262**, 264–275 (2013).